JOURNAL OF GEOPHYSICAL RESEARCH, VOL. 114, A02306, doi:10.1029/2008JA013719, 2009

Investigating the relationships among the South Atlantic Magnetic Anomaly, southern nighttime midlatitude trough, and nighttime Weddell Sea Anomaly during southern summer

Ildiko Horvath[1] and Brian C. Lovell[1,2]

Received 2 September 2008; revised 25 November 2008; accepted 4 December 2008; published 12 February 2009.

[1] This study utilized the multi-instrument data of the Defense Meteorological Satellite Program to investigate the evening/nighttime topside ionosphere during the 1996/1997 southern summer. A series of regional surface maps were constructed and permitted the tracking of the topside ionosphere's plasma density features, plasma composition, thermal structures, and vertical and horizontal plasma flows. These maps tracked a complete nighttime Weddell Sea Anomaly (WSA) and strong horizontal plasma flows that registered the high-conductivity regions of the South Atlantic Magnetic Anomaly (SAMA). These regions developed over the southeastern Pacific, just equatorward of the WSA, and over the South Atlantic. A heavy-ion stagnation trough developed poleward of the SAMA affected regions. Thus, the trough appeared on the WSA's equatorward side. During periods of increasing magnetic activity, the plasmapause was the WSA's poleward boundary. A statistical study modeled the trough's magnetic activity dependence and revealed a strong east-west hemispherical difference that was due to the SAMA effects. When the AE6 was 0 nT, the trough appeared at $(57.49 \pm 2.82)^\circ$S (geomagnetic) over the southwestern hemisphere. Owing to the SAMA's special electrodynamic effects, the trough developed at lower latitudes, $(42.39 \pm 3.04)^\circ$S, over the southeastern hemisphere. Meanwhile, the plasmapause occurred at $\sim(62.5 \pm 4)^\circ$S, and the WSA's peak appeared at $\sim(56.2 \pm 4)^\circ$S. Hence, there was a $\sim 20^\circ$ (lat) separation between the trough and the plasmapause over the southeastern hemisphere. Between 210°E and 330°E (geographic), the WSA filled this gap. With increasing magnetic activity, the trough in the SAMA affected regions moved poleward at a rate of $(0.0157 \pm 0.004)^\circ$S/nT. Elsewhere, it had a $(0.0196 \pm 0.002)^\circ$S/nT equatorward movement.

Citation: Horvath, I., and B. C. Lovell (2009), Investigating the relationships among the South Atlantic Magnetic Anomaly, southern nighttime midlatitude trough, and nighttime Weddell Sea Anomaly during southern summer, *J. Geophys. Res.*, *114*, A02306, doi:10.1029/2008JA013719.

1. Introduction

[2] High-latitude ionospheric $\mathbf{E} \times \mathbf{B}$ convection, created by the interaction of geomagnetic field (**B**) and cross-polar electric field (**E**), has a crucial role in the maintenance of the polar ionosphere and in the formation of the *F* region midlatitude or main trough, a marked plasma depletion appearing at subauroral latitudes in both hemispheres [*Muldrew*, 1965; *Moffett and Quegan*, 1983; *Rodger et al.*, 1992]. When the dawn-to-dusk **E** field and the corotation field are comparable and oppose each other, this $\mathbf{E} \times \mathbf{B}$ convection gives rise to plasma stagnation regions with a slow eastward plasma flow from dusk through midnight to dawn [*Knudsen*, 1974]. As the plasma spends its whole residence time in darkness in such stagnation regions, it becomes greatly depleted through ionic recombination and causes the development of both the morning and the evening troughs [*Brinton et al.*, 1978; *Senior et al.*, 1987; *Hedin et al.*, 2000]. Because of the nature of this process, the deepest troughs occur just on the nightside of the sunrise and sunset terminators [*Rodger et al.*, 1992]. At F region heights, a plasma density depletion related to the trough indicates a low O^+ constituent of the ionospheric plasma [*Knudsen*, 1974; *Moffett and Quegan*, 1983; *Rodger et al.*, 1992]. Although the recombination processes are sufficient to produce low electron concentration, other processes such as plasma escape along the magnetic field lines by the upward flow of H^+ in the polar winds can also act to decrease the O^+ content and can contribute to the rate of decay of the *F* region plasma [*Schunk et al.*, 1976]. In the equatorial plane, there is a boundary between this ionospheric O^+ depletion and the plasmasphere, known as the plasmapause. Its ionospheric signature, a sharp plasma density gradient [*Moffett and Quegan*, 1983; *Rodger et al.*, 1992], is often called drop-off [*Tsurutani et al.*, 2004; *Horvath*, 2007]. Modeling

[1]SAS, School of Information Technology and Electrical Engineering, University of Queensland, Brisbane, Queensland, Australia.
[2]National Information and Communications Technology Australia, University of Queensland, Brisbane, Queensland, Australia.

0148-0227/09/2008JA013719$09.00

[*Quegan et al.*, 1982] and experimental investigations [*Rodger and Pinnock*, 1982; *Smith et al.*, 1987], regarding the relationship of the trough with the plasmapause, revealed that the plasmapause maps to the equatorward side of the midlatitude trough in the early evening hours and to the poleward edge in the morning hours. Proven experimentally by global observations [*Yizengaw and Moldwin*, 2005; *Yizengaw et al.*, 2005], it is now confirmed that during periods of increasing magnetic activity the trough and the plasmapause occur on the same magnetic field line.

[3] There are considerable differences between both the two polar convection patterns [*Leonard et al.*, 1995], and the northern and southern midlatitude troughs [*Rodger et al.*, 1992]. One major cause is the ~24°-offset between the southern magnetic dip and geographic poles that is twice as large as the northern offset (~12°) [*Leonard et al.*, 1995]. While the northern trough is mostly a nighttime feature observed regularly during winter and equinox [*Moffett and Quegan*, 1983], the southern trough regularly occurs during the early afternoon/midafternoon hours and in all seasons, as the Macquarie Island (154.9°E; 54.5°S; geographic) observations of *Mallis and Essex* [1993] suggested.

[4] There are several factors that are responsible for the formation of the trough such as the magnetospheric electric field, the precipitation of soft electrons at the poleward boundary [*Aladjev et al.*, 2001], and the geomagnetic **B** field's magnitude, inclination and declination [*Karpachev et al.*, 1994; *Karpachev and Afonin*, 2004]. The equatorward trough wall, a density drop, is an important part of the trough that defines the boundary between the midlatitude and the subauroral ionosphere [*Prolss*, 2007]. Therefore, its features such as magnitude and gradient are strongly dependent on the state of the midlatitude ionosphere.

[5] Significant longitudinal variations in the distribution of ionospheric plasma at low latitudes and midlatitudes are controlled by field-aligned plasma transport and chemical processes. Owing to the spatial variability of ionospheric **E** field and geomagnetic **B** field, the equatorial vertical $\mathbf{E} \times \mathbf{B}$ drift induced movement also varies, and the following field-aligned plasma flow is modulated by a variable wind transport moving the plasma along the magnetic field lines to altitudes of different recombination rates. Over the South Atlantic, where the geomagnetic **B** field is anomalously low ($\sim 22.8 \bullet 10^3$ nT [*Trivedi et al.*, 2005]) and the ionospheric **E** field can be unusually strong because of the high conductivity of the South Atlantic Magnetic Anomaly (SAMA), the ionospheric plasma is highly changeable during both magnetically quiet times [*Abdu*, 2005; *Abdu et al.*, 2005] and disturbed periods [*Biqiang et al.*, 2007]. Quiet time northern-southern hemispherical differences are particularly evident in the American longitude sector, where there is a large 11° offset (in geographic latitude; see global magnetic field line maps of this study) between the geographic and magnetic dip equators. South of the SAMA, in the southeastern Pacific and South Atlantic Antarctic regions, the midlatitude (geomagnetic) F2 layer is illuminated all day in summer and receives only limited sunlight in winter. The magnetic field lines are unusually widely spaced there that makes the field-aligned plasma transport unusual [*Clilverd et al.*, 1991]. These extreme conditions result in the development of an inverted daily plasma density pattern at equinoxes and in summer. Detected in the ionosonde data, recorded at Faraday (65.25°S, geographic; 53.7°S, geomagnetic), the nighttime maximum is larger than the daytime minimum, and the phenomenon is known as the Weddell Sea Anomaly (WSA) [*Dungey*, 1961; *Clilverd et al.*, 1991]. *Pinnock* [1985] detected the midlatitude trough in the Faraday ionogram data mainly at nights, except in summer.

[6] However, the ionosonde data provide only a limited data coverage around the station, and the limited observational results could lead to misleading conclusions. An example is the size of the WSA. Space-based TOPEX radar altimetry, providing over-the-ocean data coverage between 66°N and 66°S geographic latitudes, was utilized recently to detect the almost complete image of the WSA [*Horvath and Essex*, 2003a; *Horvath*, 2006]. These studies revealed the much larger size of both the nighttime and the daytime WSA features than was previously thought by other researchers on the basis of their ground-based ionosonde observations. However, the limitation of the TOPEX radar data to 66°S latitude usually prevents the detection of the southern edge of the WSA. Some observations still indicate that during periods of increasing magnetic activity, the plasmapause forms its poleward boundary [*Horvath and Essex*, 2003a]. Furthermore, in the highly structured midlatitude region, there are various electron density enhancements and depletions. Therefore, electron density measurements only are not adequate to identify the midlatitude trough, which is an electron density depletion created by an O^+ content depletion [*Rodger et al.*, 1992], with high certainty, particularly in the WSA region. Because of these limitations of the TOPEX TEC data, the WSA and its vicinity, the trough and the plasmapause, have never been investigated before.

[7] The aim of this study is to utilize the multi-instrumental measurements of the Defense Meteorology Satellite Program (DMSP) that cover nearly the entire globe between 81°N and 81°S geographic latitudes in order to track the entire nighttime WSA for defining its equatorward and poleward boundaries, the southern midlatitude trough, the plasmapause, and the plasma environment of these features. Another major goal is to utilize a large database to investigate statistically the relations of these features and their longitudinal variations in order to find out the influence of the SAMA on them.

2. Data and Methodology

[8] Spacecraft of the Defense Meteorological Satellite Program (DMSP) are placed on a 96° inclined and ~105-min polar orbit, and carry built-in ion, electron and scintillation (SIESS) detectors [*Hairston et al.*, 1997]. These provide various in situ plasma measurements of the topside ionosphere at an altitude range of 850–870 km, and between 81°N and 81°S geographic latitudes. Each orbit is made up of an ascending and a descending pass. Each spacecraft of the current DMSP fleet completes around 14 orbits each day in a certain local time configuration (see details given by *Horvath* [2006]).

[9] This study's database was collected by the F12 spacecraft along its 562 ascending passes that registered 562 trough detections during the 1996/1997 southern summer. In Figure 1a, the longitudinal distribution of this database is shown. Over the southern hemisphere, these

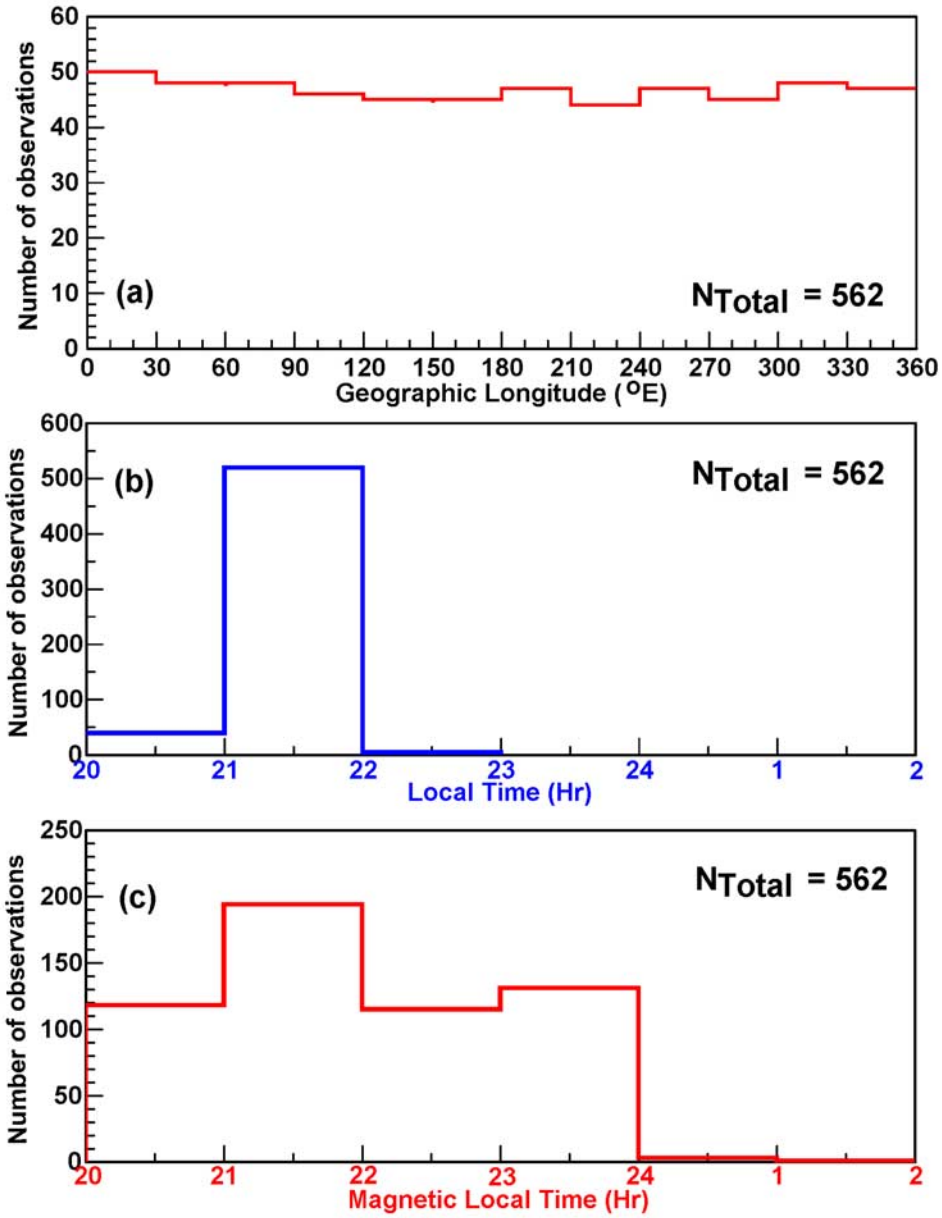

Figure 1. (a) The longitudinal distribution of the 562 trough detections is shown. (b and c) Two histograms indicate the LT and MLT distribution of the 562 midlatitude trough detections.

passes were completed during the local nighttime hours. In Figures 1b and 1c, the LT and MLT distribution of the trough detections are illustrated with two histograms. At trough latitudes, the local time varied only between 21 LT and 22 LT. However, the MLT showed a larger variation between 20 MLT and 24 MLT.

[10] A set of measurements, such as ion density (Ni, i^+/cm^3), electron and ion temperature (Te and Ti; in °K), upward and horizontal plasma drift (V_Z and V_Y; in m/s) permitting the computation of upward and horizontal plasma fluxes (F_Z and F_Y; in [$i^+/(cm^2$ s)]), and fractional amounts of O^+ and H^+ (indicated as [O^+] and [H^+], respectively), was chosen. How reliable the DMSP data are depends on the plasma composition. The relatively high (>15%) light-ion concentrations ([H^+] and [He^+]) are a major problem in the operation of the Retarding Potential Analyzer (RPA) and Ion Drift Meter (IDM) that are designed to operate in a predominantly O^+ environment. As the light-ion concentrations increase, the data quality decreases. Apart from the composition effects, the accuracy of drift data can also be compromised by the satellite posture. *Hartman and Heelis* [2007] found satellite position related uncertainties in equatorial vertical drift measurements varying between 70 m/s and 140 m/s. In this study, all the measurements related to the trough and nighttime WSA were from a predominantly O^+ environment, where the light-ion concentrations were relatively low. Moreover, the vertical and horizontal drift measurements were utilized only to compute the plasma flux values in order to demonstrate the underlying physical processes. Thus, even if some uncertainties

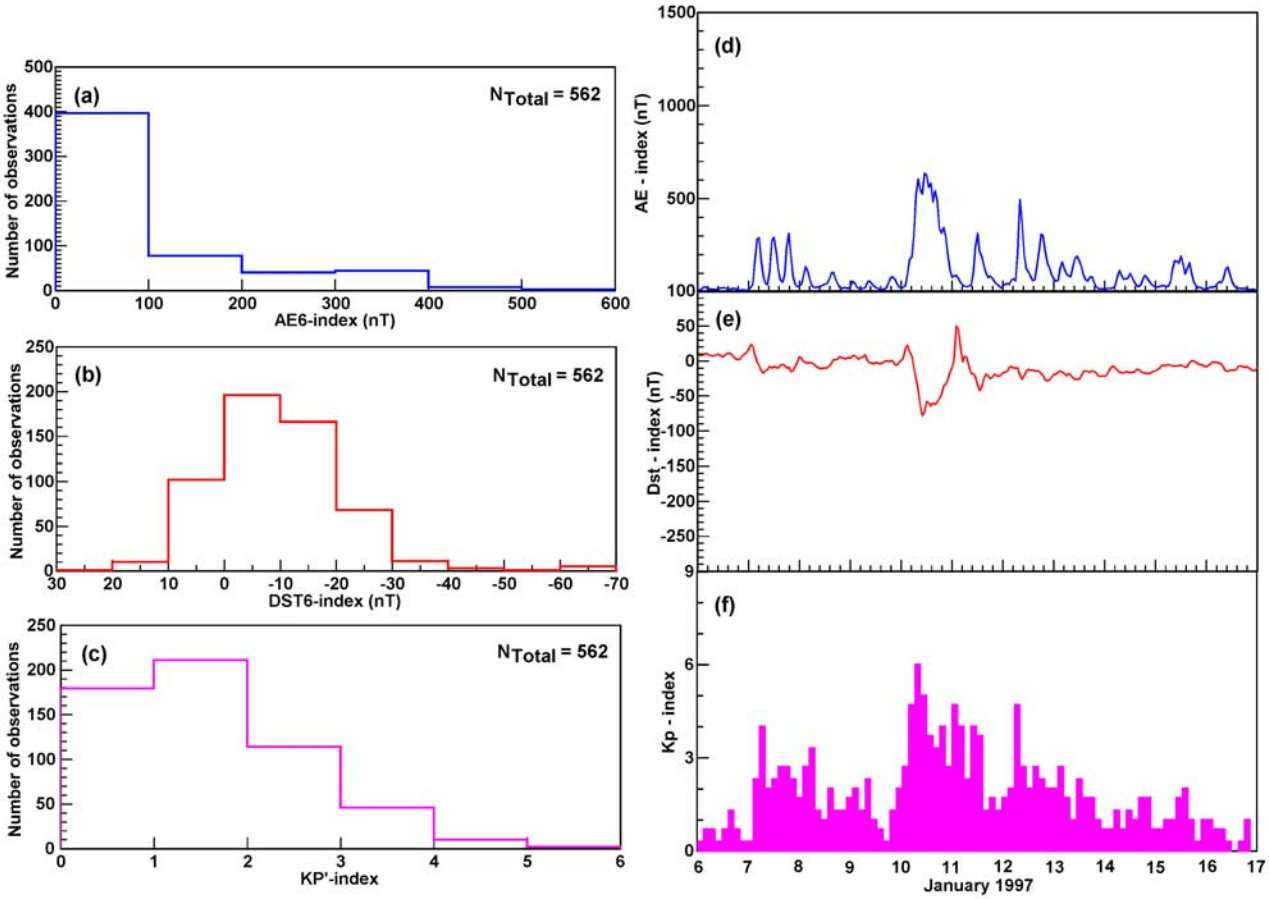

Figure 2. Three histograms illustrate the trough detections' magnetic activity distribution probed with the (a) AE6, (b) DST6, and (c) Kp′ indices. The (d) AE, (e) Dst, and (f) Kp indices depict the geomagnetic nature of the southern summer period of 6–16 January 1997.

spoiled the drift velocity values, the flux data still provided reliable and useful information to track plasma stagnations, and the WSA- and SAMA-related vertical and horizontal plasma flows.

[11] Several algorithms were designed to compute the universal (UT) and local (LT) times in decimal hours, to split each orbit track into ascending and descending passes, and to name these passes according to their orbit numbers (see details given by *Horvath* [2007]). For this study, data from the ascending passes were plotted in geographic and geomagnetic latitudes, and provided observations in a varying LT and MLT frame. An innovative mapping technique was also developed and applied to the DMSP database to bin the data into 2°(lat) × 4°(lon) cells, and to map the binned data across the two hemispheres. These maps tracked areas and regions, as seen in the time-dependent spatial coordinate system of the DMSP-F12 spacecraft. Owing to space constraints, only one map series is illustrated in this article.

3. Observational Results and Interpretations

3.1. Geomagnetic Conditions

[12] The underlying magnetic conditions of the 1996/1997 southern summer were monitored with the averaged AE and Dst, called AE6 and Dst6, indices. Introduced by *Werner and Prolss* [1997] and utilized by *Prolss* [2006, 2007], the significance of AE6 index is that it is based on the AE index of which has a well-defined physical meaning and that it takes the ionosphere's "memory effect" into account. It can be computed as [*Prolss*, 2006]

$$\mathrm{AE6} = \frac{\sum_{i=0}^{6} \mathrm{AE}(\mathrm{UT} - \mathrm{i[h]})\mathrm{e}^{-\mathrm{i}}}{\sum_{\mathrm{i}=0}^{6} \mathrm{e}^{-\mathrm{i}}} \qquad (1)$$

This study not only adopted the use of AE6 index, but also subjected the Dst index to such an averaging procedure (defined by equation (1)) producing the Dst6 index. The 3-hourly Kp index has not only a low time resolution, but an ill-defined physical meaning [*Prolss*, 2007]. Owing to the Kp index's logarithmic nature, an averaged Kp data could not be produced, but the Kp′ index, the largest Kp value during the previous 12 h, was utilized. Since the previous studies of *Werner and Prolss* [1997] and *Prolss* [2007] obtained the best magnetic activity correlation of the trough wall's location for the AE6 index, this study has adopted their method and utilized the AE6 index for its modeling study. However, to probe the magnetic activity level, all three indices were used. In Figure 2, the statistical distribution of the magnetic activity level, probed with the AE6 index (see Figure 2a), Dst6 index (see Figure 2b) and Kp′

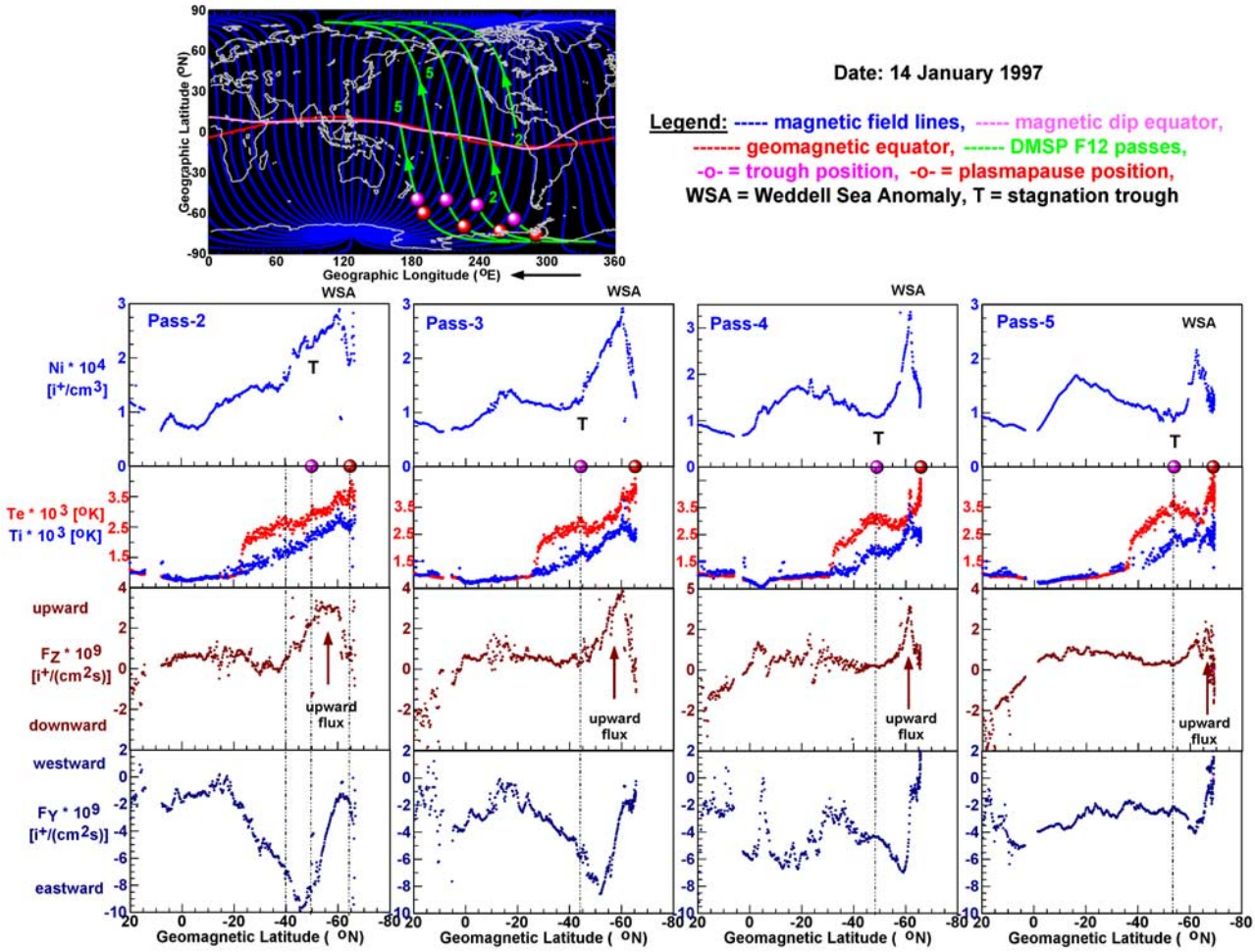

Figure 3. (top) The global map illustrates the ground tracks of the F12 passes shown below, the magnetic field lines, and the magnetic and dip equators. (bottom) Four plasma density (Ni), electron/ion temperature (Te/Ti), vertical plasma flux ($\pm F_Z$ = upward/downward (i.e., away/toward the Earth)) and horizontal plasma flux ($\pm F_Y$ = westward/eastward at low latitudes and midlatitudes, and south/north where the spacecraft turns) line plots show the midlatitude trough, the nighttime WSA, the Ni drop-off indicating the plasmapause, the related thermal structures, and the plasma circulations over the South Pacific during the magnetically mild local nighttime hours of 14 January 1997. In the first column, the locations of the nighttime WSA's equatorward and poleward boundaries and the trough are marked by dotted lines for tracking the related characteristic Te/Te and plasma flow features. For clarity, only the trough locations are marked by dotted lines in the following columns.

index (see Figure 2c), is illustrated. Most of the trough detections were made under magnetically quiet conditions, when the AE6 index was $\leq$100 nT, the Dst6 was between 10 nT and -30 nT, and the Kp′ index was $\leq$2.

[13] An 11-day period, extending from 6 to 17 January 1997, was chosen for presentation. Its magnetic nature is illustrated in Figures 2d–2f by utilizing the AE, Dst and Kp indices. There was a small magnetic storm on 10 January when the AE index reached 636 nT, the minimum Dst index was -78 nT, and the maximum Kp index was 6. A detailed description of its geomagnetic events is given by *Horvath* [2007]. Before (6–9 January) and after (13–16 January) the storm, the magnetic conditions were quiet and medium disturbed. These are indicated by the Kp index that was only occasionally larger than ~3+ and by the Dst index that did not drop lower than -30 nT.

3.2. Latitudinal Profiles of the Nighttime Topside Ionosphere

[14] Utilizing the Ni, Te, Ti, F_Z and F_Y data, a series of latitudinal profiles (geomagnetic) were constructed and are shown in the Figures 3–6. These line plots are utilized to demonstrate the spatial variations of the trough and the nighttime WSA, and to describe their plasma environment. In each of Figures 3–6, a global map showing the ground tracks of the F12 passes providing the data, with the modeled magnetic field lines and different equators, is also illustrated.

[15] Figure 3 is constructed for the South Pacific and for the quiet day of 14 January with a series of non-field-aligned line plots. As the global map indicates, these passes are positioned almost perpendicular to the magnetic field lines at midlatitudes. Each Ni profile depicts a complete

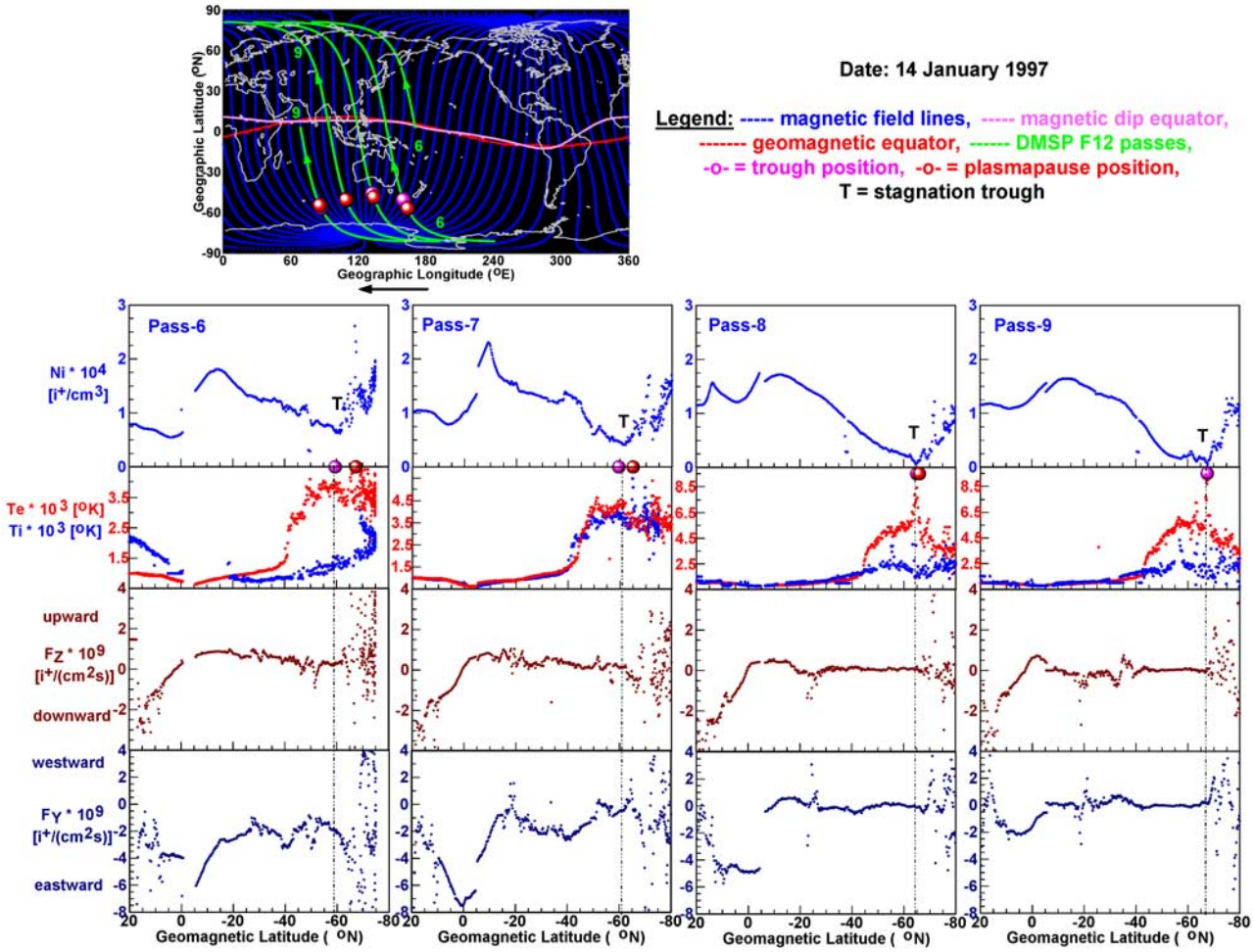

Figure 4. (top) As for Figure 3. (bottom) The various line plots show the midlatitude trough and a small section of the aurora, the related thermal structures, and the plasma circulations in the Australian sector and over the Indian Ocean during the magnetically mild local nighttime hours of 14 January 1997.

cross section of the nighttime WSA. It appears as a plasma density enhancement, relative to the ionosphere around it. The Ni line plot series demonstrate how it became better developed toward its center, which developed at around 240°E; 55°S (geographic). This is consistent with the TOPEX TEC investigation of *Horvath* [2006] covering a period of the 1996/1997 southern summer. Although the TOPEX radar data could detect only the equatorward side and the peak of the nighttime WSA, its spatial variation could still be investigated and its center could be identified in the radar data. These Ni profiles also depict that the nighttime WSA's poleward boundary, imaged as a prominent Ni drop-off, was the plasmapause. Its location is also indicated by a dotted line in the first column. There, the Te plots tracked maximum electron temperatures forming a subauroral Te peak. Ring current particles are the major source of this heat that becomes transferred from the magnetosphere to the topside ionosphere along the magnetic field lines creating a Te peak at the plasmapause and a subpeak at the trough [*Brace and Theis*, 1974; *Schunk and Nagy*, 1978; *Kozyra et al.*, 1986; *Brace et al.*, 1988; *Prolss*, 2006, 2007]. In an independent way, all the plasmapause detections were also confirmed by the relevant spectrogram images showing the low-latitude edge of the electron precipitation and thus indicating a plasmapause [*Newell et al.*, 1996]. As demonstrated with the F_Z line plots, there were maximum vertical upward flows in the nighttime WSA region that very accurately marked its latitudes. These upward plasma flows are the signature of the equatorward directed meridional neutral winds that moved the plasma up along the magnetic field lines and kept the ionization at greater altitudes where the recombination rate was lower. During this quiet period, the trough was tracked at different regions of the nighttime WSA. As the last three passes (3–5) show, the trough developed on the equatorward edge of the nighttime WSA, between 40°S and 55°S (geomagnetic), over the southeastern Pacific. Because of the already low plasma densities there, the trough appeared to be quite small in the Ni plots. This made it difficult to identify the trough in the Ni data, but the elevated Te and Ti, and the well defined plasma stagnation, as the rapid eastward plasma flow suddenly slowed down, proved its existence. Elevated ion temperatures also indicate rapid convections [*Sojka et al.*, 1981]. In this low plasma density region, where the trough appeared, both the elevated electron temperatures and the elevated ions temperatures formed well defined

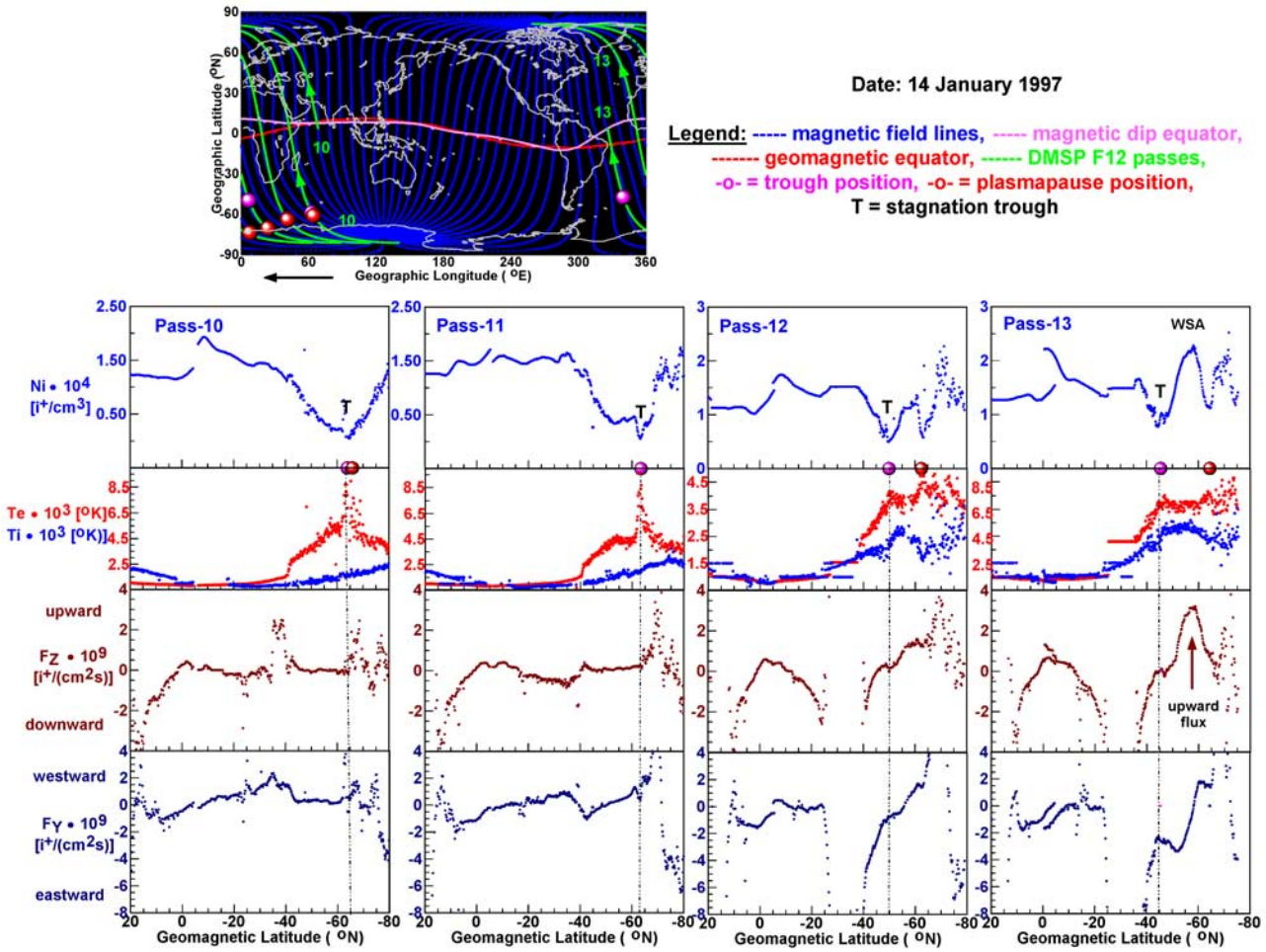

Figure 5. (top) As for Figure 3. (bottom) The various line plots show the midlatitude trough, the nighttime WSA, a small section of the aurora, the related thermal structures, and the plasma circulations in the African sector and over the South Atlantic during the magnetically mild local nighttime hours of 14 January 1997.

subpeaks, and thus marked the trough minimum and the equatorward boundary of the nighttime WSA. However, when the trough developed in the high plasma density region of the WSA (see pass 2 in first column), the trough-related Te and Ti subpeaks were not that obvious. The trough-related Te subpeak was obscured by the Te subpeak marking the Ni-depletion at the equatorward boundary of the nighttime WSA. Both of their locations are marked by dotted lines (see first column). Owing to the low plasma densities there, the conduction heating increased. All the F_Y plots tracked the strong horizontal eastward plasma flows that developed in the southeastern Pacific section of the SAMA region (see details in sections 3.3 and 4.2). These plots also show the rapid departure of the horizontal plasma flows from corotation that is the effect of these strong SAMA related horizontal eastward plasma flows on the lower-latitude plasma circulation. These eastward plasma flows maximized close to the trough, while the stagnation occurred at the trough minimum. In this longitude sector, the poleward edge of the trough was created by the solar produced ionization of the nighttime WSA. As the conduction heating decreased, owing to the high plasma densities, the Te became a minimum at WSA latitudes. Meanwhile, the Ti maximized where the eastward plasma flow was fastest owing to the increased **E** field and weak geomagnetic **B** field that gave rise to a rapid **E** × **B** convection. Another heat source for ions was the ion-neutral friction [*Schunk and Sojka*, 1982]. These F_Y and Ni detections of the trough are very similar to the observations of *Spiro et al.* [1978].

[16] Figure 4 illustrates the southern trough and its plasma environment in the Australian longitude sector and over the Indian Ocean, on the quiet day of 14 January. In these longitude sectors, the offset between the different equators is in the northern hemisphere (see global map). Thus, geomagnetic midlatitudes are situated at lower geographic latitudes. Therefore, the F12 passes could track a large section of the aurora on the poleward side of the trough. As the global map shows, the F12 passes became increasingly field aligned over the southern hemisphere. According to these line plot series, the trough appeared on the bottom of a low plasma density region, at ~60°S (geomagnetic), with the plasmapause that is indicated as a small Ni drop-off, on its poleward side. Because of the small offset between the trough minimum and the plasmapause, a single

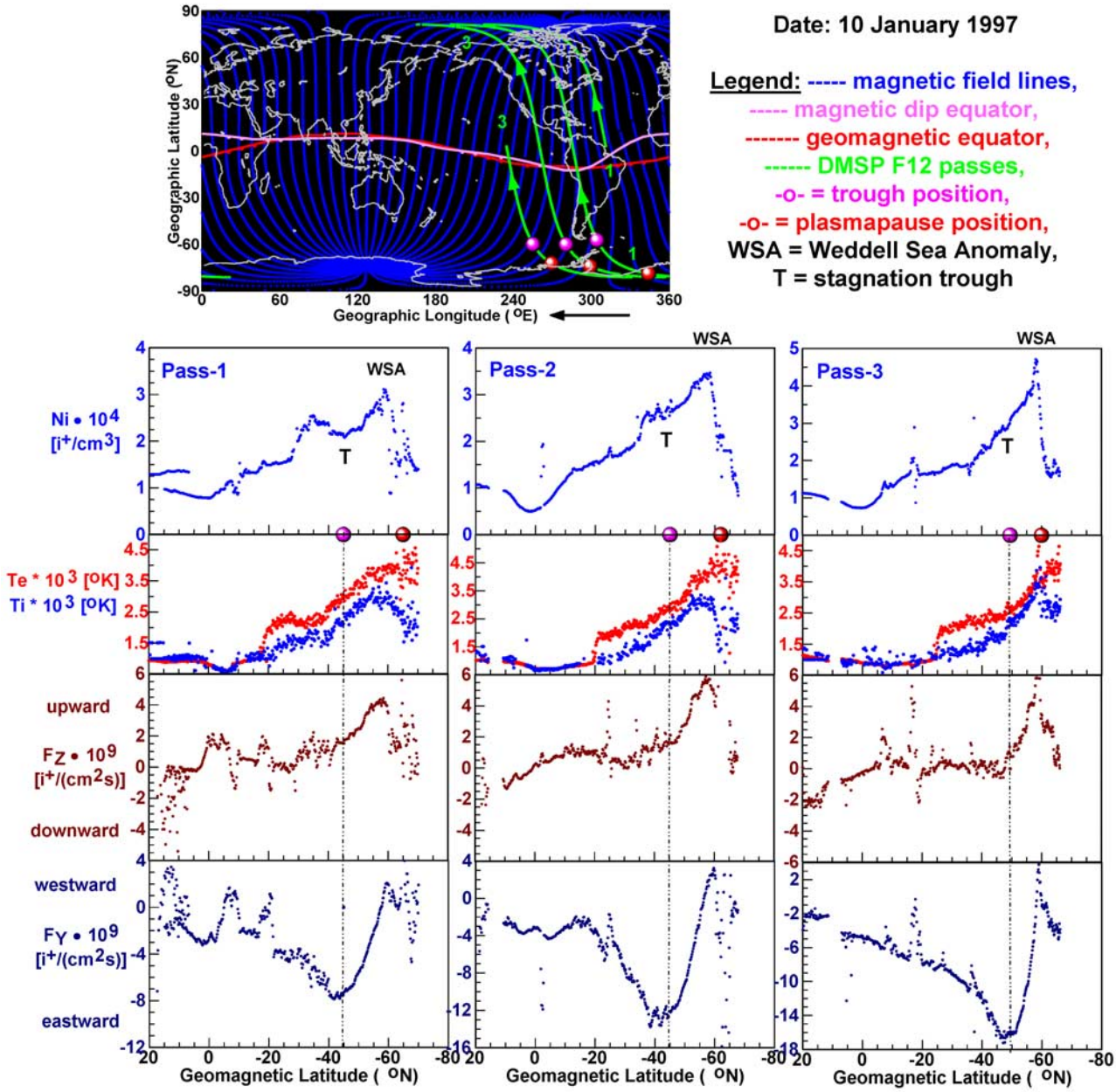

Figure 6. As for Figure 3 but during the magnetically disturbed local nighttime hours of 10 January 1997.

Te peak marked their common position. As the passes became increasingly field aligned, the Te plots show less scatter and clearly illustrate how the Te decreased in the aurora region. These field-aligned detections (see passes 8–9), showing the trough and the ionospheric signature of the plasmapause (the Ni drop-off), and the modeled magnetic field lines provide scientifically meaningful evidence that the observed trough and plasmapause were situated on the same magnetic field line during a period of increasing magnetic activity when the flux tubes were filled by plasma. It is noted here that *Yizengaw and Moldwin* [2005] and *Yizengaw et al.* [2005] proved the same without utilizing any modeled magnetic field lines. Meanwhile, the Ti plots tracked minimum ion temperatures at trough latitudes over the Indian Ocean. This could be due to the presence of the weak convections there. Supporting this suggestion, the F_Y plots show the stagnation of the horizontal eastward plasma flows at significantly lower flow values than in the South Pacific section of the SAMA affected region that was illustrated in Figure 3. At midlatitudes, the field-aligned F_Y detections of passes 8 and 9 depict the corotating midlatitude region, equatorward of the trough. Under magnetically quiet conditions, the midlatitude ionospheric plasma corotates with the Earth. As *Anderson* [1976] explained, during quiet times, the relative east-west drifts are small, compared to the corotational velocity, and create small horizontal plasma flows that allow the plasma to corotate with the Earth.

[17] Figure 5 shows the trough in the African longitude sector (passes 10–11) and over the South Atlantic (passes 12–13) on the quiet day of 14 January. In the African sector, magnetic latitudes are situated at similar geographic latitudes because of the small offset between the different equators. Over the Atlantic, where the magnetic equator is in the southern hemisphere, southern magnetic midlatitudes are at higher geographic latitudes. According to the global map, the F12 passes became increasingly field aligned over the southern hemisphere. In the African sector, the trough developed at ~65°S (geomagnetic). These trough detections are very similar to the previously described detections that were provided by two F12 passes (8–9; see details above). However, over the Atlantic, the F12 passes tracked the South Atlantic section of the SAMA region, where the eastward plasma flows dramatically increased owing to the special electrodynamic conditions (see details in sections 3.3 and 4.2). Two field-aligned passes (12–13) tracked the trough at 50°S (geomagnetic) and the profound plasma stagnation occurring poleward of the dramatically increased eastward plasma flows. At trough latitudes, these passes tracked a well developed subauroral Te subpeak indicating increased heat conduction and a Ti peak indicating the suddenly increased plasma convection. Each of these two passes also detected a well developed solar produced ionization peak on the poleward side of the trough. In the African sector (see pass 12), the smaller enhancement could be the signature of a "cliff," a remnant ionization of the decaying photoionization [*Sharp*, 1966]. Over the South Atlantic (see pass 13), the enhancement is considerably larger. Indicated by the strong upward plasma flows, this is the eastern edge of the nighttime WSA. At these two enhancements, the elevated ion temperatures indicate frictional heating from the rapid relative motion of the ions and neutrals. Poleward of these plasma enhancements, the plasmapause developed that was followed by a small section of the aurora. Because of these plasma enhancements, there was a large offset (~20.64° (geographic) measured along the magnetic field line) between the stagnation trough and the plasmapause (see pass 13). This field-aligned detection also illustrates their occurrence on the same magnetic field line during this increasing magnetic activity period.

[18] Figure 6 depicts a set of line plots constructed for the southeastern Pacific and southwestern Atlantic, for the stormy day of 10 January. A detailed study on the reaction of the nighttime WSA to this storm was carried out recently [*Horvath*, 2007]. These plots show the nighttime WSA and the trough in the South Pacific section of the SAMA region (see details above). Owing to the storm, the nighttime WSA appeared to be better developed than during the quiet period. Meanwhile, the trough developed between 45°S and 50°S (geomagnetic), in the high plasma density region of the nighttime WSA, but the plasmapause remained at ~60°S. Because of the high plasma densities, the presence of the trough is not obvious in the Ni line plot and there is only a minor Te subpeak (see pass 2) indicating its location. However, the F_Y plots show very clearly the stagnation of the eastward plasma flows, and thus help to locate the signature of the trough in the Ni, Te and Ti data. Here, in the southeastern Pacific section of the SAMA region, the maximum eastward plasma flows were significantly larger (~16 • 10^9 [i^+/(cm^2 s)]) during the storm than during the quiet period (~10 • 10^9 [i^+/(cm^2 s)]).

3.3. Regional Surface Maps of the Nighttime Topside Ionosphere

[19] Figure 7 illustrates a series of Ni, Te, Ti, [O^+] and [H^+] maps prepared with the data covering the period of 6–17 January 1997. According to the LT variation (see also section 2), the local time varied with latitude from ~2 LT at 80°S (geographic) through 21 LT at the geographic equator to 17.5 LT at 80°N. Thus, almost the entire topside ionosphere mapped was in the local nighttime sector. However, there were daytime conditions over the southeastern Pacific and the South Atlantic Antarctic region because of the constant solar illumination received by the F region. The affected area was clearly defined by the high plasma densities creating a nighttime WSA at ~23 LT. Because of the averaged values utilized for plotting, these maps depict an average behavior of the topside ionosphere during that 11-day period. As was mentioned before, these maps depict areas and regions as seen in the time-dependent spatial coordinate system of the DMSP-F12 spacecraft. For a more detailed analysis, the trough and plasmapause locations, tracked on the days of 10 January (when the storm was on) and 14 January (when the magnetic conditions returned to normal after the storm), were plotted over the maps.

[20] The ion density (Ni in i^+/cm^3) map of Figure 7a depicts an average plasma density distribution of the topside ionosphere over the northern winter and southern summer hemispheres. The most outstanding ionospheric features tracked are a southern midlatitude trough, a nighttime WSA and a nighttime equatorial ionization enhancement over the Atlantic. As a depletion relative to the ionosphere around it, the trough appeared quite well developed between 15°E and 150°E, over the Indian Ocean and in the Australian sector (4 • 10^3 i^+/cm^3; in brown, 2 • 10^3 i^+/cm^3; in dark brown). Opposite to the trough feature, the nighttime WSA appeared between 210°E and 330°E as a substantial plasma enhancement (31 • 10^3 i^+/cm^3; in red), relative to the ionosphere around it, where the *F* region was illuminated. The nighttime ionization enhancement between 310°E and 350°E, over the dip equator in the Atlantic sector, is the signature of the evening variation of the equatorial anomaly (see details given by *Horvath and Essex* [2003b]). As indicated by the investigations of the individual satellite passes of this 11-day period, the trough's geographic location changed considerably. Over the southwestern hemisphere, between around 15°E and 120°E (geographic), it developed at lower latitudes on 10 January, when the magnetic storm was on, and at higher latitudes during the quiet times such as on 14 January. There, the average Ni map tracked both the storm time and the quiet time trough positions. In order to get a perspective on where the trough developed during these periods, the positions of the trough minimum and the plasmapause were plotted over the various maps for these two days. The two (second and third) Ni maps with the overplots reveal how accurately the average Ni map tracked both the quiet time and the storm time troughs, and that the plasmapause developed very close to the trough minimum between 30°E and 120°E. Although, the Ni map itself shows very clearly how the trough became shallower (7 • 10^3 i^+/cm^3; in yellow) over the middle of the South Pacific (at ~180°E; geographic), it could not track it

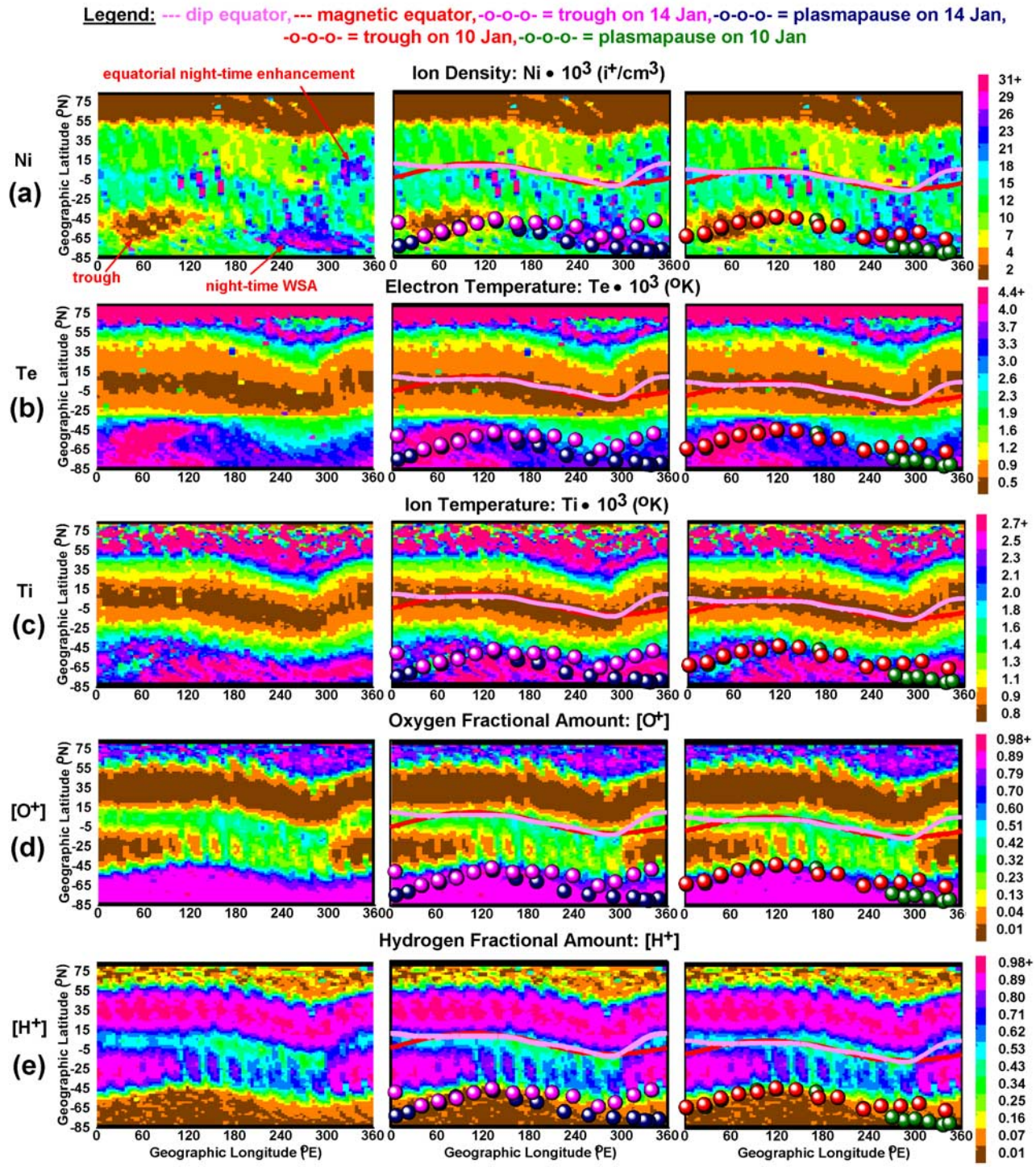

Figure 7. The regional maps depict the spatial distribution of (a) ion density (Ni in 10^3 • i^+/cm^3), (b) electron temperature (Te in 10^3 • °K), (c) ion temperature (Te in 10^3 • °K), and the fractional amounts of (d) $[O^+]$ and (e) $[H^+]$ in the topside ionosphere during 6–17 January 1997.

further than ~180°E, over the southeastern Pacific. This is because of the averaged Ni values utilized for plotting. In the binning process, the lower Ni values, indicating the trough, got smoothed out. However, the signature of a shallow quiet time trough (7 • 10^3 i^+/cm^3; in yellow) over the South Atlantic is clearly visible. Another interesting feature revealed by the overplots is the increasingly large offset between the trough minimum and the plasmapause, starting at ~180°E, slightly away from the western edge of the nighttime WSA. Thus, the WSA filled most of the gap between them during these periods. Consequently, the trough developed on the equatorward edge of the nighttime

WSA and the plasmapause on its poleward edge. What caused this split will be revealed below (see sections 4.3–4.4).

[21] The electron temperature (Te in °K) map (see Figure 7b) and the ion temperature (Ti in °K) map (see Figure 7c) depict the thermal structures of the nighttime topside ionosphere. Between 0°E and 120°E, there are maximum (4.4 • 10^3 °K in red) electron temperatures in the regions of the southern trough and aurora. Eastward of these hot spots, the higher Te (4.0 • 10^3 °K in pink) values indicate the position of the plasmapause and the lower Te (3.0 • 10^3 °K in dark blue) values mark the position of the trough minimum. From 120°E eastward, the high ion temperatures (2.1 • 10^3 °K in dark blue) mark the positions of the quiet time trough minimum, while the higher Ti values (2.5 • 10^3 °K in pink and 2.7 • 10^3 °K in red) mark the plasmapause. These interpretations are demonstrated with the overplots in the second and third Te and Ti maps.

[22] The plasma chemistry of the nighttime topside ionosphere is depicted by the [O^+] and [H^+] maps (see Figures 7d and 7e), illustrating how the fractional amount of O^+ and H^+ varied spatially in an opposite phase during the period studied. In the southern hemisphere, there is a continuous band of O^+ depletion (0.70 in dark blue) that is the signature of the midlatitude trough. The coincidence of the storm time trough position with this O^+ depletion is evident from the overplots (see third [O^+] map). However, in the high [O^+] region (0.89 in pink), there are traces of [O^+] depletion (0.70 in dark blue) that indicate the development of the quiet time trough at higher latitudes (see second [O^+] map). These [O^+] and [H^+] maps clearly show that at ~850 km altitude, the O^+ was still the dominant ion in the summer hemisphere at trough and higher latitudes. On the basis of the study of *Zhao et al.* [2005], this can be explained with regard to the rapid flux tube volume increases with increasing latitude. The downward diffusion of H^+ from the protonosphere and its charge exchange reaction ($H^+ + O \leftrightarrow O^+ + H$) were able to maintain the high O^+ concentration [*Zhao et al.*, 2005]. Below the heavy ion/light ion transition height, the [H^+] map tracked a depletion (0.01 in dark brown) in the southern hemisphere, where the quiet time plasmapause developed (see second [H^+] map). Consequently, this H^+ depletion is not the signature of a light-ion trough that occurs at altitude where the H^+ is the dominant ion [*Moffett and Quegan*, 1983; *Rodger et al.*, 1992]. However, there is evidence [*Horwitz et al.*, 1990] that the light-ion structure of the topside ionosphere sometimes resembles to that of the plasmasphere. Assuming the existence of such a resemblance, this H^+ depletion can be the topside ionospheric signature of a light-ion trough. Meanwhile, during periods of increasing magnetic activity, the plasmapause appeared at slightly lower latitudes, along the equatorward edge of this light-ion depression. Recently, *Anderson et al.* [2008] utilized the H^+ line plots to track the light-ion trough and to define from such measurements the location of the ionospheric projection of the plasmapause. It is interesting to note, that in both hemispheres, the [O^+]-depleted (0.01 in dark brown) and [H^+]-rich (0.89 in pink; 0.99 in red) regions are situated at magnetic midlatitudes, and show significant longitudinal variations at southern latitudes. In good agreement with the results of *Zhao et al.* [2005], these composition maps indicate that at low sunspot numbers, such as in 1996 and 1997, H^+ was the predominant ion composition at midlatitudes in the nighttime sector. This was possibly created by the loss of ions at lower altitudes at local nighttime hours, when the downward plasma diffusion of H^+ prevailed at the satellite altitude and decreased the upward plasma flows induced by upward pressure gradient forces [*Zhao et al.*, 2005; *Kil et al.*, 2006]. The longitudinal variation of these constituents was due to various transport processes created by hemispheric and interhemispheric neutral winds, diffusion along the magnetic field line and $\mathbf{E} \times \mathbf{B}$ drifts [*Zhao et al.*, 2005, and references therein]. Depending on their seasonal, local time and longitudinal variations, the equatorward neutral winds and summer-to-winter interhemispheric plasma flows at midlatitudes could impede more or less the downward nighttime plasma diffusion [*Zhao et al.*, 2005; *Kil et al.*, 2006]. A longitudinal uniformity in the winter northern hemisphere is evident, as the weak neutral winds, owing to the small declination angles, introduced little longitudinal variations. Meanwhile, there are well defined longitudinal variations in the southern summer hemisphere. There, the lowest O^+ concentrations (0.01 in dark brown) developed over the SAMA region (300°E–30°E) where possibly the special electrodynamic effects accelerated this downward diffusion the most. There were also low O^+ concentrations (<0.23) in the African sector and over the Indian Ocean, between 30°E and 120°E, where the equatorward directed neutral winds were weak and thus could not impede the downward diffusion. Medium high [O^+], between 0.23 and 0.42, were registered over the southeastern Pacific (190°E–300°E), where the most effective equatorward winds retarded the plasma diffusion the most. *Kil et al.* [2006] also detected the most depleted [O^+] in the same longitude sectors utilizing the DMSP data collected by the F15 spacecraft during the 2003 southern spring period of 27 September–1 October. As the second and third [O^+] maps show with the overplots, in the SAMA region (300°E–30°E), the quiet time trough developed close to the poleward edge of this most depleted [O^+] region, and further away from it during the storm.

[23] Figure 8 illustrates the F_Z and F_Y plasma flux maps that tracked the vertical plasma diffusions (see Figure 8a) and the horizontal plasma flows (see Figure 8b), respectively. According to the DMSP data format, the ±plasma flux (F_Z) values indicate vertical plasma flows away/toward the center of the Earth. In the horizontal direction, the ±plasma flux (F_Y) values indicate westward/eastward plasma flows at low latitudes and midlatitudes (geographic) and south/north plasma flows at high latitudes (>75°S; geographic) where the spacecraft turns. Thus, these maps provide significant information on the vertical and horizontal plasma transports that played a crucial role in the development of the nighttime WSA and the trough, respectively. These maps' most outstanding features are explained in the following section. In the nighttime WSA region, the F_Z map (see Figure 8a) tracked maximum vertical upward plasma diffusions (4.00 • 10^9 [i^+/(cm^2 s)] in red) between 230°E and 330°E. Driven by the strong equatorward directed neutral winds, these diffusions were responsible for transporting the plasma along the magnetic field lines to higher altitudes, where the recombination rates were low (see details given by *Horvath* [2006]). However, these diffusions gradually lost intensity (0.73 • 10^9 [i^+/(cm^2 s)] in blue) at trough latitudes, over the southwestern Pacific (between

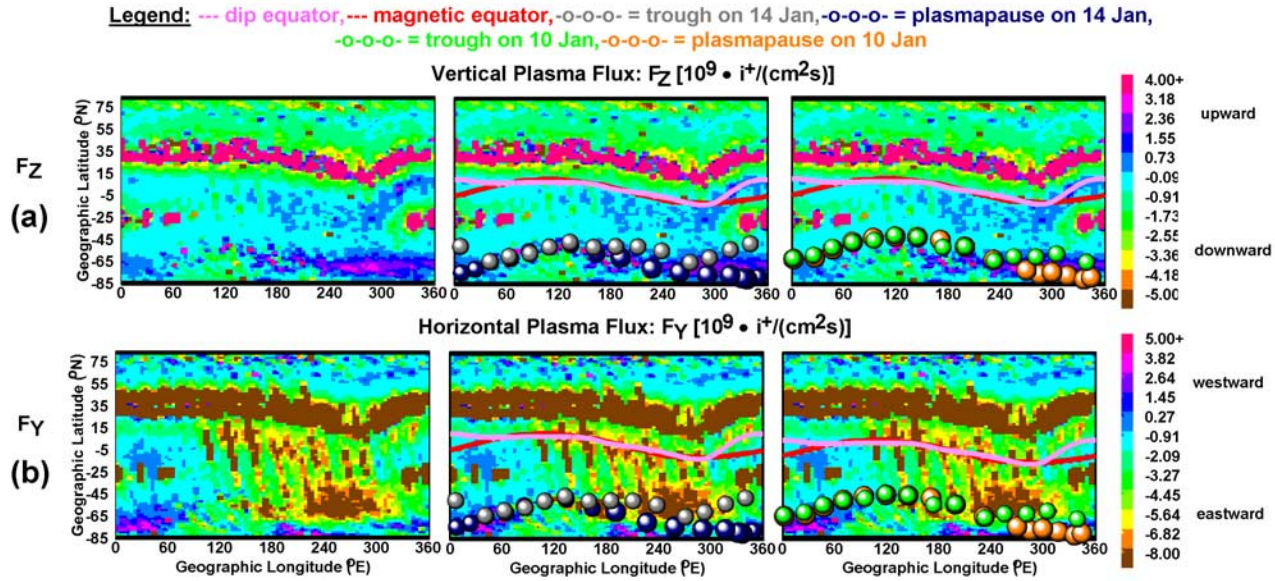

Figure 8. The regional maps depict the spatial distribution of (a) vertical plasma flux (F_Z in $\{10^9 \bullet [i^+/(cm^2\ s)]\}$) and (b) the horizontal plasma flux (F_Y in $\{10^9 \bullet [i^+/(cm^2\ s)]\}$) in the topside ionosphere during the period of 6–17 January 1997. ($\pm F_Z$ = upward/downward (i.e., away/toward the center of the Earth); $\pm F_Y$ = westward/eastward at low latitudes and midlatitudes (geographic) and south/north at high latitudes (>75°S) where the spacecraft turns.)

150°E and 220°E) and in the Australian longitude sector (between 70°E and 150°E. This indicates the longitudinal variation of the equatorward directed neutral winds. Meanwhile, the F_Y map (see Figure 8b) tracked maximum horizontal plasma flows ($5.00 \bullet 10^9$ $[i^+/(cm^2\ s)]$ in red) at plasmapause latitudes, between 0°E–90°E and 300°E–360°E (see second and third F_Y maps). Furthermore, the F_Y map tracked two well defined regions, where the eastward horizontal plasma flows maximized ($-8.00 \bullet 10^9$ $[i^+/(cm^2\ s)]$ in dark brown). The first one was a well defined circular-shaped region (between 200°E and 310°E) situated equatorward of the nighttime WSA. The second one was a smaller region (between 330°E and 15°E) that was aligned with the dip equator over the South Atlantic. These two regions were the SAMA affected regions that developed over the southeastern Pacific and South Atlantic, respectively, during this 11-day period. Known from the works of *Abdu* [2005] and *Abdu et al.* [2005], there are special electrodynamic conditions in the SAMA region. These increased the conductivity gradient during the postsunset hours (~21.5 LT) of the studied period. Thus, the neutral winds blew more intensively across the sunset terminator, enhanced the electric field (**E**) and the resultant increased drift drove the eastward plasma flows most rapidly (see more details in section 4.3). These increased eastward plasma flows, the signatures of the SAMA's special electrodynamic effects, were tracked by the F_Y map. The SAMA affected region, north of the nighttime WSA, was significantly better developed than the region over the South Atlantic. There were two reasons for this. This better developed region covered a larger section of the sunset terminator, which was situated just north of the nighttime WSA, and the winds were stronger in the WSA longitude sector, owing to the large (45°) southerly inclination and large (40°) easterly declination (see details given *Horvath* [2006]). It was along their poleward boundaries of these regions, where the trough developed, as the overplots (see second and third F_Y maps) indicate. However, westward from the nighttime WSA, over the southwestern hemisphere, the eastward plasma flows at trough latitudes gradually decreased to around zero ($0.27 \bullet 10^9$ $[i^+/(cm^2\ s)]$ in blue). These detections indicate that the plasma stagnation (demonstrated in section 3.2), causing the development of the trough, occurred at increasingly high eastward plasma flows toward the WSA, as plasma stagnation-related plasma flows maximized in the SAMA affected regions. At these maximum eastward plasma flows, caused by the special electrodynamic effects of the SAMA region, the plasma stagnations gave rise to the development of a trough close to and in the high-plasma density region of the nighttime WSA. These were demonstrated with a series of line plots in the previous section.

3.4. Statistical Results

[24] Figure 9's error bar plots show the statistical results obtained from the 562 trough, 200 WSA and 500 plasmapause detections. In Figure 9a, the trough's average LT and MLT variations in geographic longitude is shown. While the LT remained constant at ~22 LT, the MLT oscillated between 21 MLT and 23 MLT. Their maximum difference was ~(1.45 ± 0.4) hours. How the average statistical locations of the trough minimum, nighttime WSA peak and plasmapause varied in the grid of geographic latitudes and longitudes is illustrated in Figure 9b. Apparently, the trough developed equatorward of the nighttime WSA and the plasmapause occurred poleward of the WSA. Their spatial variation in the grid of geomagnetic latitudes and

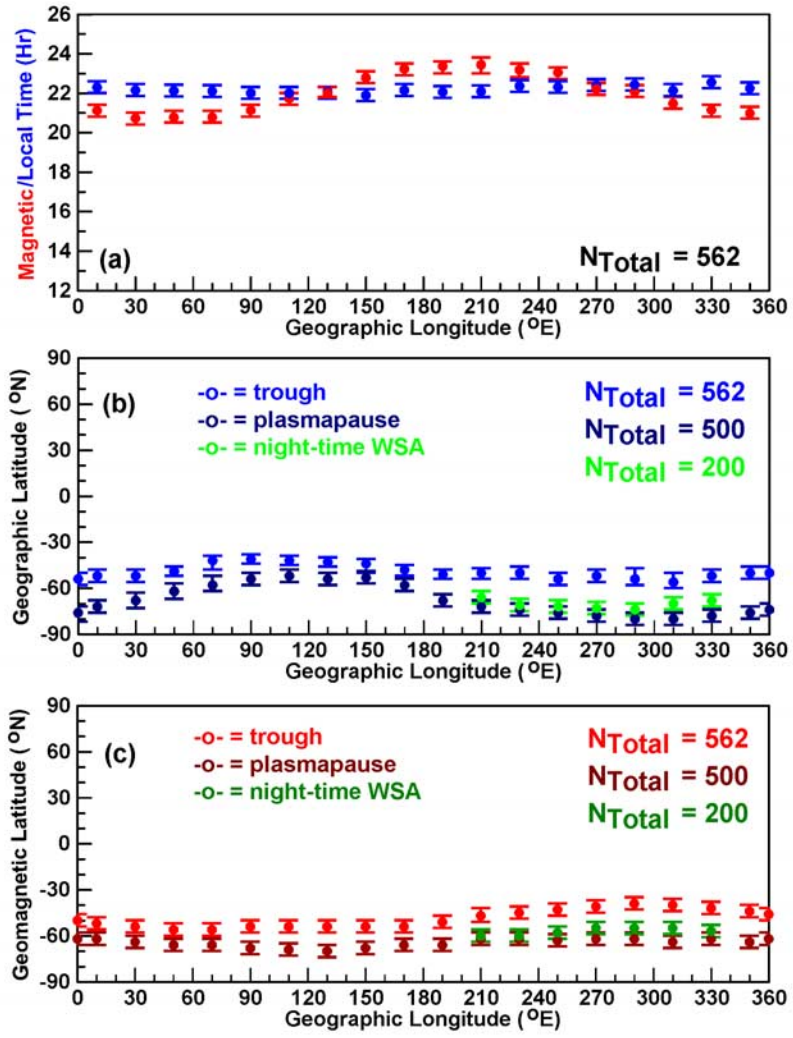

Figure 9. The first error bar plot illustrates the local time (LT) and magnetic local time (MLT) variations of the trough detections in geographic longitude. (a) While the LT remained almost constant at around 22 LT, the MLT oscillated between 20 MLT and 24 MLT. (b) The second error bar plot shows the spatial variations of the average positions of the trough, WSA peak, and plasmapause in the grid of geographic latitudes and longitudes. (c) In the third error bar plot, these features' positions are shown in the grid of geomagnetic latitudes and geographic longitudes. The trough's development at lower magnetic latitudes over the southeastern hemisphere is obvious.

geographic longitudes is shown in Figure 9c. From this plotting style, it becomes evident that the trough developed at higher geomagnetic latitudes (at ~(54 ± 4)°S; geomagnetic) between 90°E and 170°E over the southwestern hemisphere, and significantly closer to the equator (at ~(40 ± 4)°S) between 250°E and 330°E over the southeastern hemisphere, poleward of the SAMA region and equatorward of the nighttime WSA. Meanwhile, the plasmapause developed at ~(67.5 ± 4)°S between 50°E and 190°E, and at ~(62.5 ± 4)°S between 210°E and 350°E. Because of this small, ~5° latitude difference between the eastern and western hemispheres, the plasmapause location exhibited a nice magnetic alignment that is also obvious from the relevant error bar plot of Figure 9b. Showing also a nice magnetic alignment, the WSA peak developed mainly at ~(56.2 ± 4)°S between 210°E and 330°E.

[25] This strong east-west hemispherical difference in the trough location warranted to conduct a separate statistical investigation of the southern trough for each hemisphere. Its main aim was to correlate the trough location (indicated as MLAT) with the level of magnetic activity that was probed with the AE6 index accounting for the ionosphere's "memory effect" [*Werner and Prolss*, 1997; *Prolss*, 2006, 2007]. In Figure 10 the error bar plots illustrate the correlation results obtained for the western (see Figure 10a) and eastern (see Figure 10b) longitude sectors. For each sampling interval a median value and a ± error was obtained from the scatterplots. Then, a line of best fit for the median values was obtained via a linear regression analysis. For each regression line, the associated a and b parameters defining the Y intercept and the gradient, respectively, were identified with a ± error indicated as Δa and Δb, respectively. From these

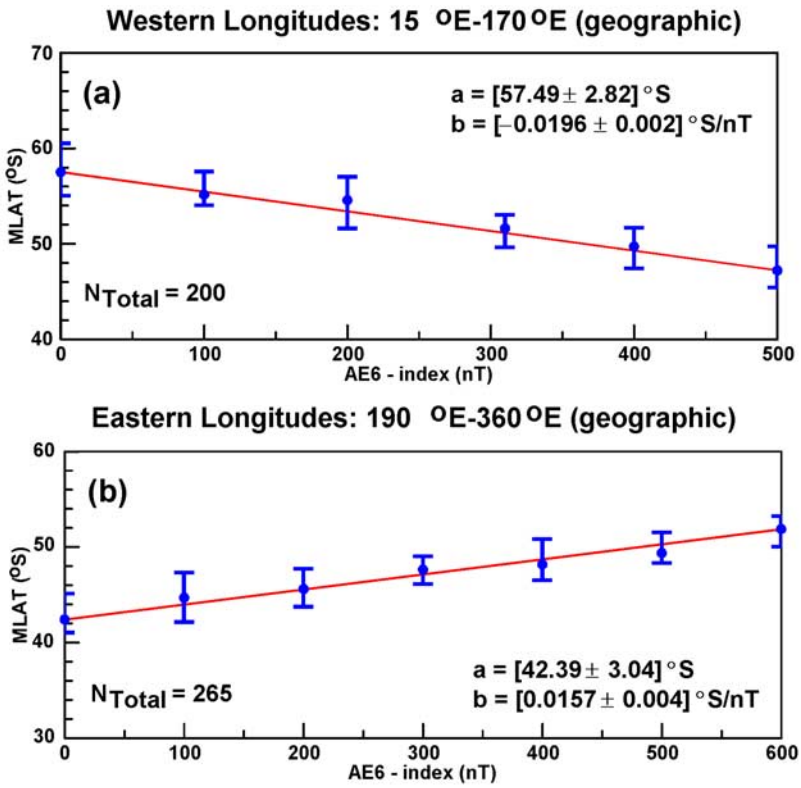

Figure 10. The error bar plots show the statistical variation of the summer nighttime trough position in magnetic latitude (MLAT) with the level of magnetic activity probed with the AE6 index over the (a) southwestern and (b) southeastern hemispheres.

parameters, the magnetic activity dependency of the trough minimum was modeled utilizing the standard formula of $y(x) = a \pm b(x)$. These models for the southwestern hemisphere (see equation (2)) and for the southeastern hemisphere (see equation (3)) are

$$\mathrm{MLAT(AE6)[^\circ S]} = 57.49[^\circ \mathrm{S}] - 0.019[^\circ \mathrm{S/nT}]\mathrm{AE6} \quad \Delta a = \pm 2.82[^\circ \mathrm{S}] \quad \Delta b = \pm 0.002[^\circ \mathrm{S/nT}] \tag{2}$$

$$\mathrm{MLAT(AE6)[^\circ S]} = 42.39[^\circ \mathrm{S}] + 0.016[^\circ \mathrm{S/nT}]\mathrm{AE6} \quad \Delta a = \pm 3.04[^\circ \mathrm{S}] \quad \Delta b = \pm 0.004[^\circ \mathrm{S/nT}] \tag{3}$$

According to these regression lines, over the southwestern hemisphere, the trough developed between at ~57.60 ± 2.82)°S (geomagnetic) and moved to lower latitudes, closer to the equator, as the level of magnetic activity increased. The rate of movement is indicated by the negative gradient value of 0.019 [°S/nT]. Over the southeastern hemisphere, the trough developed at lower latitudes, at ~(42.39 ± 3.04)°S. The rate of movement was similar, 0.016) [°S/nT], but the positive sign indicates that the trough moved away from the magnetic equator, toward higher latitudes, as the magnetic activity level increased. *Prolss* [2007] correlated the northern-hemisphere winter trough with the AE6 index showing an equatorward movement, as the magnetic activity level increased. Compared with this study's southwestern hemisphere trough correlation result, the northern winter nighttime trough appeared at higher geomagnetic latitude, at ~70.2°N, that could be a seasonal effect, and moved equatorward with a rate of −0.018°N/nT that is very similar to this study's value of (−0.0196 ± 0.002)°S/nT.

4. Discussion

[26] To overcome the two-dimensional limitation of the individual DMSP passes, the simultaneous in situ plasma measurements, providing continuous data coverage, were mapped over the two hemispheres. The resultant high-resolution maps had the ability to image, almost globally, the topside ionosphere's morphology, thermal structure, plasma composition and plasma circulations. Coupled with the 562 individual line plots and the modeled magnetic field lines, the various large-scale plasma density features and their characteristics were investigated. Results revealed that during the 1996/1997 southern summer, two large-scale heavy-ion features dominated the southern topside ionosphere: the nighttime midlatitude trough and the nighttime WSA. The trough developed on the nighttime WSA's

equatorward side and during periods of increasing magnetic activity the plasmapause on the anomaly's poleward side.

4.1. First Detection of an Entire Nighttime WSA and Its Plasma Environment

[27] Demonstrated with a map series, the complete image of a nighttime WSA was tracked for the first time with its plasma environment. At ~23 LT, it appeared at ~(56.2 ± 4)°S (geomagnetic) between 210°E and 330°E (geographic) longitudes during magnetically quiet times. Its Ni image showed a strong magnetic alignment, which reflects the spatial variation of the underlying physical mechanisms that were controlled by the magnetic declination, inclination and field intensity. From the recent TOPEX TEC investigations [*Horvath*, 2006, 2007] and related CTIP model studies [*Zou et al.*, 2000; *Rishbeth et al.*, 2000], the basic physical mechanisms taking place over the southeastern Pacific are reasonably well understood. However, an entire nighttime WSA feature has never been detected, and its plasma environment and its relation to other ionospheric features have never been investigated statistically before.

[28] Tracking the most intensive vertical upward plasma flows in the nighttime WSA region, the F_Z map has demonstrated the paramount importance of the thermospheric neutral winds in its development. Regarding its plasma chemistry, the $[O^+]$ and $[H^+]$ maps have revealed its high O^+ and low H^+ contents, and that the midaltitude heavy-ion (Ni-O^+) trough appeared on its equatorward side, in a low plasma density region, and the topside ionospheric signature of the light-ion (H^+) trough occurred on its poleward side. These results are quite surprising, because previous trough investigations in the WSA region, at Faraday [*Rodger and Pinnock*, 1982; *Pinnock*, 1985], utilizing ground-based ionosonde data, did not detect the midlatitude trough in summer. The trough's absence was explained with the filling effects of the significant solar produced ionization that created the nighttime WSA. During periods of increasing magnetic activity of the 1996/1997 southern summer, the plasmapause occurred on the poleward side of the nighttime WSA. There was a strong correspondence found between the topside ionospheric signature of the light-ion trough and the plasmapause that can be explained with reference to the basic characteristics of the plasmapause and light-ion trough: they are essential features in the H^+ distribution of the topside ionosphere and magnetosphere [*Rodger et al.*, 1992].

[29] Regarding the nighttime WSA's thermal structures, its equatorward boundary was marked by elevated subauroral ion and electron temperatures, and its poleward boundary was indicated by the highest subauroral electron temperatures. As these Te signatures are closely associated with the heavy-ion (Ni-O^+) midlatitude trough and the plasmapause [*Kozyra et al.*, 1986; *Prolss*, 2006, 2007], these also suggested, in an independent way, the appearance of the trough and the plasmapause, respectively.

4.2. Southern Midlatitude Trough and Its Relation to the Nighttime WSA

[30] Tracking the stagnating plasma, trapped between the regions eastward corotating plasma flow and westward convection flow, occurring in darkness and creating electron density depletions larger than expected [*Knudsen*, 1974; *Whalen*, 1989], confirmed that the heavy-ion trough was a stagnation trough. Over the southwestern hemisphere, between 15°E and 170°E, the plasma stagnation occurred at the slowest horizontal eastward plasma flow in the night side (see Figures 4 and 5). Thus, the stagnating plasma decayed in darkness or in limited sunlight, as it spent its whole prolonged residence time in there. This led to the development of a large stagnation trough. However, the trough became increasingly less developed over the southeastern hemisphere, between 180°E and 330°E (see Figure 3), as the conditions changed rapidly between 180°E and 210°E. In the nighttime WSA region, the trough reached its least developed form. There, the prevailing daytime conditions, due to the illuminated F2 layer, in its close vicinity and the strong equatorward directed neutral winds caused its rapid refilling. However, the horizontal eastward plasma flows dramatically increased toward and maximized in the nighttime WSA region. This created the most profound plasma stagnation events along the nighttime WSA's equatorward edge. But, the stagnating plasma could decay only little, owing to its short residence time in limited sunlight on the equatorward edge of the nighttime WSA, or in broad daylight, when it developed closer to the WSA peak. Thus, the close occurrence of these two very different ionospheric features, the stagnation trough and the nighttime WSA, demonstrated a very strong competition among the underlying physical processes, which reached their extremes over the southeastern Pacific (between 200°E and 310°E) because of the special electrodynamic conditions existing there (see more details in section 4.3). Those competing underlying processes were the stagnation of the horizontal eastward plasma flow that depleted the residing plasma via recombination, and the constant production of solar ionization that was subjected to the strongest vertical lifting effects of equatorward neutral winds filling up the existing plasma depletions.

4.3. SAMA Region and Its Relation to the Stagnation Trough and the Nighttime WSA

[31] In the F2 layer, the velocity (**V**) of **E** field driven plasma motion, occurring perpendicular ($\perp$) to the geomagnetic field (**B**) lines, can be estimated as $\mathbf{V}_\perp = (\mathbf{E} \times \mathbf{B})/B^2$ [*Kendall and Pickering*, 1967]. At high latitudes, this estimation models a horizontal plasma motion, which is usually termed "plasma convection." The horizontal variation of this convection velocity, via the variation of the **B** field and **E** field intensities, creates the corresponding variations of the electrodynamic processes, which contribute to the longitudinal variation of the midlatitude trough. In the SAMA affected region, where the geomagnetic field intensity is anomalously low, the plasma convection is strongest because of the weak geomagnetic magnetic field. Further, there is also an east-west conductivity gradient, which adds to the conductivity gradient developing across the sunset terminator at sunset. This increases the **E** field in the evening sector and leads to the dramatic increase of the $\mathbf{E} \times \mathbf{B}$ plasma convection [*Abdu*, 2005; *Abdu et al.*, 2005]. In this study, the F_Y map tracked the SAMA affected areas, as seen in the time-dependent spatial coordinate system of the DMSP-F12 spacecraft, very accurately by their increased $\mathbf{E} \times \mathbf{B}$ plasma convections. Although the center of the SAMA is at ~310°E; 10°S (geographic), over South

Brazil, the combination of weak **B** fields and increased **E** fields affected two separate areas: a smaller area over the South Atlantic (between 330°E and 15°E) and a larger area over the southeastern Pacific (between 200°E and 310°E). In these areas, the sunset terminator developed equatorward of the nighttime WSA that appeared between 210°E and 330°E. Thus, the SAMA played a great role via its **E** field and **B** field effects in both the development of the stagnation trough along the equatorward nighttime WSA boundary and the formation of this boundary itself. This study's statistical investigation has revealed that the southern stagnation trough's behavior showed strong east-west hemispherical differences because of the SAMA effects. Over the southwestern hemisphere, between 15°E and 170°E, away from the SAMA affected region, the trough location was primarily dependent on the level of magnetic activity. There, the trough appeared at ~58°S geomagnetic latitude and moved to lower latitudes when the activity level increased (see equation (2)). However, over the southeastern hemisphere, in the close vicinity of the SAMA region, altogether between 210°E and 15°E, the trough appeared ~10–15 geomagnetic latitude degrees lower than over the southwestern hemisphere and moved to higher latitudes when the level of magnetic activity increased (see equation (3)). *Smith et al.* [1987] also reported the rapid equatorward movement of the trough in the evening hours but did not explain it at all. As it became clear from this study, it was at that time, around sunset, when the dramatically increased conductivity over the SAMA region enhanced the **E** field. The interaction of the anomalously weak **B** field and this enhanced **E** field triggered the development of both the extremely strong convective eastward $\mathbf{E} \times \mathbf{B}$ plasma flows and the stagnation trough over the southeastern Pacific (between 210°E and 310°E) and South Atlantic (between 330°E and 15°E) at significantly lower latitudes than normally when the conductivity gradient was absent at other local times. Because of the strong SAMA effects, there was a large gap over the southeastern hemisphere between the stagnation trough and the plasmapause, and the nighttime WSA filled this gap between 210°E and 330°E.

5. Summary and Conclusion

[32] This study has investigated the nighttime WSA and the heavy-ion ($Ni\text{-}O^+$) midlatitude trough, and their relations with other essential features of the topside ionosphere such as the plasmapause. It utilized in situ multi-instrument data, collected by the DMSP-F12 spacecraft during the 1996/1997 southern summer, and the modeled magnetic field lines. The almost global regional surface maps permitted the simultaneous investigations of the variations of plasma composition, ion/electron temperature, and plasma circulation in the topside nighttime ionosphere. These maps revealed that the nighttime WSA, the heavy-ion trough, and the plasmapause were the essential features of the southern topside ionosphere at local evening/nighttime. Furthermore, the horizontal plasma flow maps, tracking maximum plasma flows over the southeastern Pacific and South Atlantic, registered the areas, as seen in the time-dependent spatial coordinate system of the DMSP-F12 spacecraft, affected by the SAMA's special electrodynamic effects. A statistical investigation was performed on the trough and resulted in the modeling its magnetic activity dependency. This complex, experimental and statistical, investigation provided the following significant findings.

[33] The heavy-ion trough was a stagnation trough that dominated with the plasmapause, during periods of increasing magnetic activity, the southwestern hemisphere where evening/nighttime conditions prevailed and the horizontal plasma convections were ordinary. The trough location was controlled by the level of magnetic activity and exhibited equatorward movements when the activity level increased. Over the southeastern hemisphere, the dominant features were the nighttime WSA, the stagnation trough and the plasmapause. While the stagnation trough developed at lower latitudes, poleward of the SAMA affected areas, and on the equatorward side of or sometimes within the nighttime WSA, the plasmapause comprised the WSA's poleward boundary during periods of increasing magnetic activity. The trough location was also controlled by the SAMA's electrodynamic effects that altered the convection paths. As a result, the trough developed ~10–15 magnetic latitude degrees closer to the equator in the vicinity of the SAMA affected areas, which occurred equatorward of the nightime WSA, and moved poleward, instead of equatorward, when the magnetic activity level increased.

[34] As a direct consequence of these peculiarities, occurring between 210°E and 15°E, the stagnation trough was separated from the plasmapause by an increasingly large offset creating a gap. This gap was partially filled by the nighttime WSA and became largest (~26° (geographic), measured along the magnetic field line) over the southeastern Atlantic, east of the nighttime WSA.

[35] The coexistence of the nighttime WSA and the stagnation trough was the net result of a fierce competition between the very different physical processes creating plasma enhancements and depletions in heavy ions. These competing processes obviously left the light-ions unaffected, as neither the nighttime WSA nor the stagnation trough left its signature in the $[H^+]$ distribution. Meanwhile, the topside ionospheric signature of the light-ion trough showed a close correspondence with the plasmapause at all longitudes, and with the stagnation trough over the southwestern hemisphere where the trough developed along the regular convection paths.

[36] **Acknowledgments.** This study was supported by a University of Queensland Postdoctoral Research Fellowship. NICTA is funded by the Australian Government's Backing Australia's Ability initiative, in part through the Australian Research Council. The authors are thankful to the DMSP project teams for the data and to M. Hairston for his advice. The AE, Dst, and Kp indices are from WDC-2 at Kyoto (http://swdcdb.kugi.kyoto-u.ac.jp).

[37] Wolfgang Baumjohann thanks the reviewers for their assistance in evaluating this paper.

References

Abdu, M. A. (2005), Equatorial ionosphere–thermosphere system: Electrodynamics and irregularities, *Adv. Space Res.*, *35*(5), 771–787, doi:10.1016/j.asr.2005.03.150.

Abdu, M. A., I. S. Batista, A. J. Carrasco, and C. G. M. Brum (2005), South Atlantic magnetic anomaly ionization: A review and a new focus on electrodynamic effects in the equatorial ionosphere, *J. Atmos. Sol. Terr. Phys.*, *67*, 1643–1657, doi:10.1016/j.jastp.2005.01.014.

Aladjev, G. A., O. V. Evstafiev, V. S. Mingalev, G. I. Mingalev, E. D. Tereshchenko, and B. Z. Khudukon (2001), Interpretation of ionospheric *F* region structures in the vicinity of ionization troughs observed by satellite radio tomography, *Ann. Geophys.*, *19*, 25–36.

Anderson, D. A. (1976), Modeling the mid-latitude *F* region ionospheric storm using east-west drift and a meridional wind, *Planet. Space Sci.*, *24*, 69–77, doi:10.1016/0032-0633(76)90063-5.

Anderson, P. C., W. R. Johnston, and J. Goldstein (2008), Observations of the ionospheric projection of the plasmapause, *Geophys. Res. Lett.*, *35*, L15110, doi:10.1029/2008GL033978.

Biqiang, Z., W. Weixing, L. Libo, and M. Tian (2007), Morphology in the total electron content under geomagnetic disturbed conditions: Results from global ionosphere maps, *Ann. Geophys.*, *25*, 1555–1568.

Brace, L. H., and R. F. Theis (1974), The behavior of the plasmapause at mid-latitudes: Isis 1 Lamgmuir probe measurements, *J. Geophys. Res.*, *79*, 1871–1884, doi:10.1029/JA079i013p01871.

Brace, L. H., C. R. Chappell, M. O. Chandler, R. H. Comfort, J. L. Horwitz, and W. R. Hoegy (1988), F region electron temperature signatures of the plasmapause based on Dynamics Explorer 1 and 2 measurements, *J. Geophys. Res.*, *93*, 1896–1908, doi:10.1029/JA093iA03p01896.

Brinton, H. C., J. M. Grebowsky, and L. H. Brace (1978), The high-latitude winter F region at 300 km: Thermal plasma observations from AE-C, *J. Geophys. Res.*, *83*, 4767–4776, doi:10.1029/JA083iA10p04767.

Clilverd, M. A., A. J. Smith, and N. R. Thompson (1991), The annual variation in quiet time plasmaspheric electron density, determined from whistler mode group delays, *Planet. Space Sci.*, *39*, 1059–1067, doi:10.1016/0032-0633(91)90113-O.

Dungey, J. W. (1961), Interplanetary magnetic field and the auroral zones, *Phys. Rev. Lett.*, *6*, 47–48, doi:10.1103/PhysRevLett.6.47.

Hairston, M. R., R. Heelis, and F. Rich (1997), Analysis of the ionospheric cross polar cap potential drop and polar ion convection patterns during the January 1997 CME events using DMSP data, *Eos Trans. AGU*, Spring Meet. Suppl., *78*(17), S264.

Hartman, W. A., and R. A. Heelis (2007), Longitudinal variations in the equatorial vertical drift in the topside ionosphere, *J. Geophys. Res.*, *112*, A03305, doi:10.1029/2006JA011773.

Hedin, M., et al. (2000), 3-D extent of the main ionospheric trough—A case study, *Adv. Pol. Atmos. Res.*, *14*, 157–162.

Horvath, I. (2006), A total electron content space weather study of the nighttime Weddell Sea Anomaly of 1996/1997 southern summer with TOPEX/Poseidon radar altimetry, *J. Geophys. Res.*, *111*, A12317, doi:10.1029/2006JA011679.

Horvath, I. (2007), Impact of 10 January 1997 geomagnetic storm on the nighttime Weddell Sea Anomaly: A study utilizing data provided by the TOPEX/Poseidon mission and the Defense Meteorological Satellite Program, and simulations generated by the Coupled Thermosphere/Ionosphere Plasmasphere model, *J. Geophys. Res.*, *112*, A06329, doi:10.1029/2006JA012153.

Horvath, I., and E. A. Essex (2003a), The Weddell Sea Anomaly observed with the TOPEX satellite data, *J. Atmos. Sol. Terr. Phys.*, *65*, 693–706, doi:10.1016/S1364-6826(03)00083-X.

Horvath, I., and E. A. Essex (2003b), Vertical $\mathbf{E} \times \mathbf{B}$ drift velocity variations and associated low-latitude ionospheric irregularities investigated with the TOPEX and GPS satellite data, *Ann. Geophys.*, *21*, 1017–1030.

Horwitz, J. L., R. H. Comfort, P. G. Richards, M. O. Chandler, C. R. Chappell, P. Anderson, W. B. Hanson, and I. H. Brace (1990), Plasmasphere-ionosphere coupling: 2. Ion composition measurements at plasmaspheric and ionospheric altitudes and comparison with modeling results, *J. Geophys. Res.*, *95*, 7949–7959, doi:10.1029/JA095iA06p07949.

Karpachev, A. T., and V. V. Afonin (2004), Variations in the structure of the high-latitude ionosphere during the March 22–23 1979 storm based on Cosmos-900 and Intercosmos-19 data, *Geomagn. Aeron.*, *44*, 60–68.

Karpachev, A. T., V. V. Afonin, and Y. Shmilauer (1994), Variation of the nighttime trough position with longitude in winter and equinox conditions: A comparison, *Geomagn. Aeron.*, *34*, 55–59.

Kendall, P. C., and W. M. Pickering (1967), Magnetoplasma diffusion at F2-region altitudes, *Planet. Space Sci.*, *15*, 825–833, doi:10.1016/0032-0633(67)90118-3.

Kil, H., R. DeMajistre, L. J. Paxton, and Y. Zhang (2006), Nighttime *F* region morphology in the low and middle latitudes seen from DMSP F15 and TIMES/GUVI, *J. Atmos. Sol. Terr. Phys.*, *68*, 1672–1681, doi:10.1016/j.jastp.2006.05.024.

Knudsen, W. C. (1974), Magnetospheric convection and the high-latitude F_2 ionosphere, *J. Geophys. Res.*, *79*, 1046–1055, doi:10.1029/JA079i007p01046.

Kozyra, J. U., L. H. Brace, T. E. Cravens, and A. F. Nagy (1986), A statistical study of the subauroral electron temperature enhancement using Explorer 2 Langmuir probe observations, *J. Geophys. Res.*, *91*, 11,270–11,280, doi:10.1029/JA091iA10p11270.

Leonard, J. M., M. Pinnock, A. S. Rodger, J. R. Dudeney, R. A. Greenwald, and K. B. Barker (1995), Ionospheric plasma convection in the southern hemisphere, *J. Atmos. Terr. Phys.*, *57*, 889–897, doi:10.1016/0021-9169(94)00070-5.

Mallis, M., and E. A. Essex (1993), Diurnal and seasonal variability of the southern hemisphere main ionospheric trough from differential-phase measurements, *J. Atmos. Terr. Phys.*, *55*, 1021–1037, doi:10.1016/0021-9169(93)90095-G.

Moffett, R. J., and S. Quegan (1983), The mid-latitude trough in the electron concentration of the ionospheric F-layer: A review of observations and modeling, *J. Atmos. Terr. Phys.*, *45*, 315–343, doi:10.1016/S0021-9169(83)80038-5.

Muldrew, D. B. (1965), *F*-layer ionization trough deduced from Alouette data, *J. Geophys. Res.*, *70*, 2635–2650, doi:10.1029/JZ070i011p02635.

Newell, P. T., Y. I. Feldstein, Y. I. Galperin, and C.-I. Meng (1996), Morphology of nightside precipitation, *J. Geophys. Res.*, *101*, 10,737–10,748, doi:10.1029/95JA03516.

Pinnock, M. (1985), Observations of a day-time mid-latitude ionospheric trough, *J. Atmos. Terr. Phys.*, *47*, 1111–1121, doi:10.1016/0021-9169(85)90029-7.

Prolss, G. W. (2006), Subauroral electron temperature enhancement in the nighttime ionosphere, *Ann. Geophys.*, *24*, 1871–1885.

Prolss, G. W. (2007), The equatorial wall of the subauroral trough in the afternoon/evening sector, *Ann. Geophys.*, *25*, 645–659.

Quegan, S., G. J. Bailey, R. J. Moffett, R. A. Heelis, T. J. Fuller-Rowell, D. Rees, and R. W. Spiro (1982), A theoretical study of the distribution of ionization in the high-latitude ionosphere and the plasmasphere: First results on the mid-latitude trough and the light-ion trough, *J. Atmos. Terr. Phys.*, *44*, 619–640, doi:10.1016/0021-9169(82)90073-3.

Rishbeth, H., I. C. F. Muller-Wodarg, L. Zou, T. J. Fuller-Rowell, G. H. Millward, R. J. Moffett, A. D. Aylward, D. W. Idenden, and A. D. Aylward (2000), Annual and semiannual variations in the ionospheric F2-layer. II. Physical discussion, *Ann. Geophys.*, *18*, 945–956, doi:10.1007/s00585-000-0945-6.

Rodger, A. S., and M. Pinnock (1982), Movements of the mid-latitude ionospheric trough, *J. Atmos. Terr. Phys.*, *44*, 985–992, doi:10.1016/0021-9169(82)90063-0.

Rodger, A. S., R. J. Moffett, and S. Quegan (1992), The role of ion drift in the formation of ionization troughs in the mid- and high-latitude ionosphere—A review, *J. Atmos. Terr. Phys.*, *54*, 1–30, doi:10.1016/0021-9169(92)90082-V.

Schunk, R. W., and A. F. Nagy (1978), Electron temperature in the F region of the ionosphere: Theory and observation, *Rev. Geophys. Space Phys.*, *16*, 355–399, doi:10.1029/RG016i003p00355.

Schunk, R. W., and J. J. Sojka (1982), Ion temperature variations in the daytime high-latitude *F* region, *J. Geophys. Res.*, *87*, 5169–5183, doi:10.1029/JA087iA07p05169.

Schunk, R. W., P. M. Banks, and W. J. Raitt (1976), Effects of electric fields and other processes upon the nighttime high-latitude *F* layer, *J. Geophys. Res.*, *81*, 3271–3282, doi:10.1029/JA081i019p03271.

Senior, C., J. R. Sharber, O. de la Beaujardière, R. A. Heelis, D. S. Evans, J. D. Winningham, M. Sugiura, and W. R. Hoegy (1987), *E* and *F* region study of the evening sector auroral oval: A Chatanika/Dynamics Explorer 2/NOAA 6 comparison, *J. Geophys. Res.*, *92*, 2477–2494, doi:10.1029/JA092iA03p02477.

Sharp, G. W. (1966), Midlatitude trough in the night ionosphere, *J. Geophys. Res.*, *71*, 1345–1356.

Smith, A. J., A. S. Rodger, and D. W. P. Thomas (1987), Simultaneous ground-based observations of the plasmapause and the *F* region mid-latitude trough, *J. Atmos. Terr. Phys.*, *49*, 43–47, doi:10.1016/0021-9169(87)90080-8.

Sojka, J. J., W. Raitt, and R. W. Schunk (1981), A theoretical study of the high-latitude winter F region at solar minimum for low magnetic activity, *J. Geophys. Res.*, *86*, 609–621, doi:10.1029/JA086iA02p00609.

Spiro, R. W., R. A. Heelis, and W. B. Hanson (1978), Ion convection and the formation of the mid-latitude *F* region ionization trough, *J. Geophys. Res.*, *83*, 4255–4264, doi:10.1029/JA083iA09p04255.

Trivedi, N. B., B. M. Pathan, N. J. Schuch, M. Barreto, and L. G. Dutra (2005), Geomagnetic phenomena in the South Atlantic anomaly region in Brazil, *Adv. Space Res.*, *36*(10), 2021–2024, doi:10.1016/j.asr.2004.09.020.

Tsurutani, B., et al. (2004), Global dayside ionospheric uplift and enhancement associated with interplanetary electric fields, *J. Geophys. Res.*, *109*, A08302, doi:10.1029/2003JA010342.

Werner, S., and G. W. Prolss (1997), The position of the ionospheric trough as a function of local time and magnetic activity, *Adv. Space Res.*, *20*(9), 1717–1722, doi:10.1016/S0273-1177(97)00578-4.

Whalen, J. A. (1989), The daytime *F* layer trough and its relation to ionospheric-magnetospheric convection, *J. Geophys. Res.*, *94*, 17,169–17,184, doi:10.1029/JA094iA12p17169.

Yizengaw, E., and M. B. Moldwin (2005), The altitude extension of the mid-latitude trough and its correlation with plasmapause position, *Geophys. Res. Lett.*, *32*, L09105, doi:10.1029/2005GL022854.

Yizengaw, E., H. Wei, M. B. Moldwin, D. Galvan, L. Mandrake, A. Mannucci, and X. Pi (2005), The correlation between mid-latitude trough and the plasmapause, *Geophys. Res. Lett.*, *32*, L10102, doi:10.1029/2005GL022954.

Zhao, B., W. Wan, L. Liu, X. Yue, and S. Venkatraman (2005), Statistical characteristics of the total ion density in the topside ionosphere during period of 1996–2004 using empirical orthogonal function (EOF) analysis, *Ann. Geophys.*, *23*, 3615–3631.

Zou, L., H. Rishbeth, I. C. F. Muller-Wodarg, A. D. Aylward, G. H. Millward, T. J. Fuller-Rowell, D. W. Idenden, and R. J. Moffett (2000), Annual and semiannual variations in the ionospheric F2-layer. I. Modelling, *Ann. Geophys.*, *18*, 927–944, doi:10.1007/s00585-000-0927-8.

I. Horvath and B. C. Lovell, SAS, School of Information Technology and Electrical Engineering, University of Queensland, Brisbane, Qld 4072, Australia. (ihorvath@itee.uq.edu.au)